Available online at www.sciencedirect.com

ScienceDirect

Energy Procedia 160 (2019) 526–533

Energy Procedia

www.elsevier.com/locate/procedia

2nd International Conference on Energy and Power, ICEP2018, 13–15 December 2018, Sydney, Australia

A performance analysis of tidal turbine conversion system based on control strategies

K.Omkar[a,]*, K.B.Karthikeyan[a], Srimathi R.[a], Nithya Venkatesan[a*], E.J.Avital[b], A.Samad[c], S.H.Rhee[d]

[a]*School of Electrical Engineering, VIT University, Chennai, India*
[b]*Queen Mary University, London, United Kingdom*
[c]*Department of Ocean Engineering, IIT Madras, India*
[d]*Naval Architecture and Ocean Engineering, Seoul National University, Seoul, Korea.*

Abstract

Energy efficient generation from renewable energy sources is of major concern nowadays. A horizontal axis marine current turbine (HAMCT) of diameter 1.9 m is modelled using the blade element momentum (BEM) scheme and the turbine output parameters are given as an input to the electrical system for a tip speed ratio (TSR) of 5 and a power coefficient of 0.4. The design aspects of a buck-boost converter with proportional integral (PI) and sliding mode controller (SMC) is investigated for HAMCT system, with the highest power output of about 15.6 kW for a water velocity of 3 m/s. A comparison between PI controller and SMC are analyzed for the tidal turbine conversion system to obtain the desired output voltage with high efficiency is discussed here. The dynamic variation on load side to be controlled with dual loop controller to regulate the output voltage and to optimize the input current. In this paper performance and resemblance of control techniques which include sliding mode controller and PI controller are analysed with step and bode plot response. The system is designed for an output voltage range of 0.38 kV to 2.4 kV which is suitable for DC microgrids. The performance of HAMCT coupled with PMSG and the power converter with a controller is modelled and designed under MATLAB/SIMULINK environment.

Selection and peer-review under responsibility of the scientific committee of the 2nd International Conference on Energy and Power, ICEP2018.

Keywords: Tidal current; PMSG; Buck-boost converter; Marine current turbine; BEM.

* Corresponding author. Tel.: +044 3993 1262.
E-mail address: kambli.omkar@gmail.com

Selection and peer-review under responsibility of the scientific committee of the 2nd International Conference on Energy and Power, ICEP2018.
10.1016/j.egypro.2019.02.202

1. Introduction

The renewable energy source includes sunlight, geothermal, wind, tides, water, biomass, etc. out of these, tides are predictable sources of energy and tidal turbines show a high potential[1]. A review of turbine systems like horizontal and vertical axis, in association with their arrangement and the qualitative relationship, was reported by Khan [2]. The Gulf of Khambhat in the west coastal line of India along with the inlet of the Arabian Sea is a potential location for the installation of the tidal energy system with an extreme tidal range that peaks to 10 m during spring tide[3][4].

Generally, tidal turbine conversion systems (TTCS) [1]use either fixed or variable speed type of generators and the variable type of generators can extract maximum power at different speeds resulting in the maximization of the hydrodynamic efficiency of the turbines[4]. Similarly, to wind energy system, TTCS consists of a PMSG, a diode bridge rectifier, a DC-DC converter which is finally connected to the DC microgrid as shown in Fig. 1.

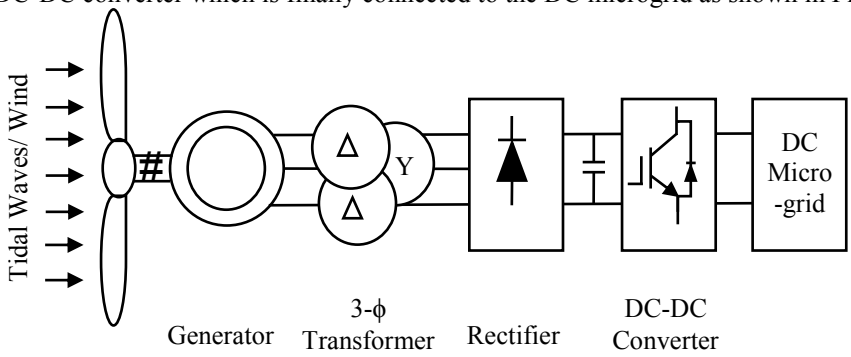

Fig. 1: Small-scale TTCS system with diode rectifier and buck-boost converter with DC micro-grid

This paper uses the modelling and control of PMSG for tidal turbine applications. In Section 2, tidal current turbine hydrodynamics and its dynamic models are explained in detail. Section 3 presents the PMSG model and its validation in association with the power rating. Section 4 discusses the design aspects of the DC-DC buck-boost converter with the controller classification. Section 5 summarizes the results and provides the controller implementation. Finally, Section 6 offers some concluding remarks and future work discussions.

Nomenclature

A	Cross-section of the turbine (m^2)
a, a'	Induction and tangential induction factors respectively
C_P	Turbine power coefficient
D	Duty cycle
$\hat{d}$	Duty cycle for controlled switching action to a buck-boost converter
f_r	Ripple frequency and ripple factor (Rf) is evaluated from output ripple without filter (Hz)
f_S	Switching frequency (kHz)
i_{ds},i_{qs}	d and q-axis Stator current (A)
Δi_L	Ripple current in inductor considered to be 10% of input current of the converter (A)
I_O	Output current of buck boost converter (A)
L_d,L_q	d and q self-inductances (H)
P	Extracted power from the flow (kW)
P_{in}	Input power from the source (kW)
R	Radius of the turbine (m), $r < 0.7R$
S	State variable trajectory
V_O	Output voltage of buck boost converter (V)
V_i, V_{rel}	Incoming velocity of the tidal current (m/s) and relative velocity (m/s) seen by segment of blade section
ΔV_C	Output voltage ripple considered to be 0.5% of output voltage (V)
V_{ph-ph}	Phase to phase voltage for Δ and Y transformer connections (V)
ρ	Water density (kg/m^3)
Ω	Rotational speed (m/s)
x, ψ	Axial and tangential directions respectively

λ_{qs} ,λ_{ds}	Stator q and d-axis flux linkages (Wb-t)
x_1, x_2, x_e	State variable for inductor current (i_L), output capacitor voltage (V_C), total tracking error
α_1, α_2	Control parameters termed as sliding co-efficient

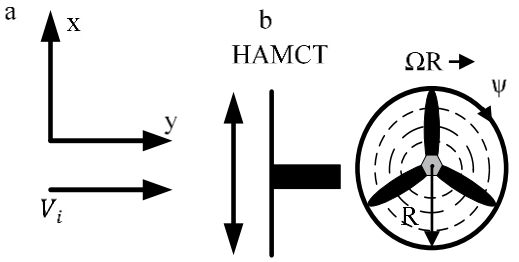

Fig. 2: (a)Schematic description of the horizontal axis marine current turbine, (b)its rotor – disc modelled using axis symmetry rings in BEM.

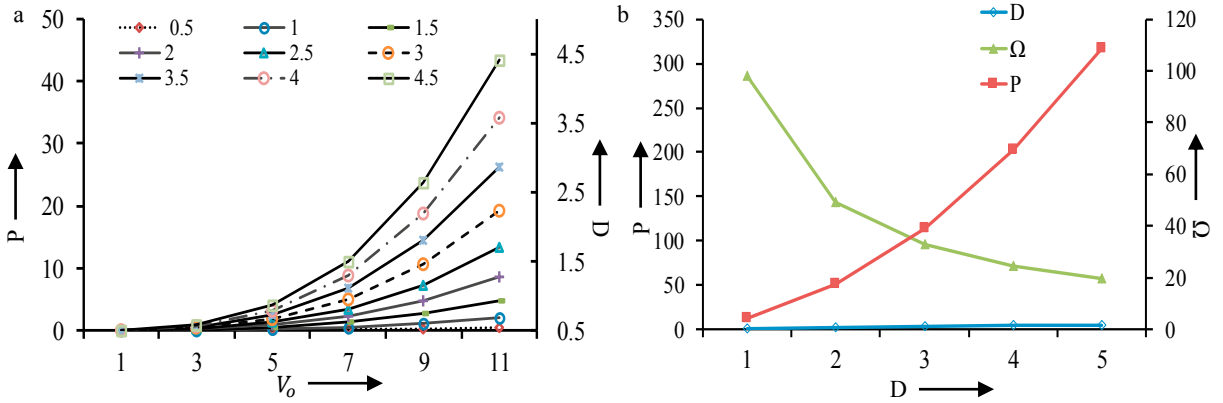

Fig. 3: a) Power variation over for a tidal velocity of 1 m/s to 11 m/s, b) Diameter variations with power, rotational frequency and speed of the rotor.

2. Tidal turbine hydrodynamics and model

Tidal hydrokinetic turbines harvest tidal energy. The power coefficient (Cp) of the turbine is defined as,

$$C_p = \frac{P}{0.5\rho V_i^3 A} \quad (1)$$

A common hydrodynamic model is the BEM technique due to its very low computational cost, while reasonably providing accurate results[4][5][6]. For this study, we assume the turbine is far enough from the water surface and other surfaces as in Fig. 2(a) and use the steady BEM approach[4]. The rotor disc is divided into rings as illustrated in Fig. 2(b), where the axial and tangential velocity seen by the segment of the blade section of that ring is;

$$V_{rel} = V_i[1 - a(r)]\hat{x} + \Omega r[1 + a'(r)]\hat{\varphi} \quad (2)$$

Once the induction factors were found then by the momentum theory the rotor power coefficient is;

$$C_p = 8\lambda_R^2 \int_{y_{low}}^{1} a'(1-a)y^3 dy\,,\ y \equiv {}^{r}/_{R} \quad (3)$$

The variation in tidal velocity and the corresponding theoretical power calculations using (2) is shown in Fig. 3(a) and (b). In this paper a 15.6 kW direct-driven turbine with 1.9 m of diameter is taken for further analysis.

3. PMSG modelling

Tidal currents are usually low in speed for which the PMSG is most extensively used to optimize the produced energy[7]. The dynamic model of a non-salient PMSG machine in a synchronous rotation is considered in a direct-quadrature reference using the park's transformation frame and an essential assumption are made[8]. Fig. 4 shows the SIMULINK diagram of the modelled PMSG in MATLAB / SIMULINK environment and the various parameter values used to model the PMSG[9].

From the reference frame circuit, the voltage equations for a synchronous generator,

$$V_{ds} = -R_s i_{ds} - \omega_r \lambda_{qs} + \frac{d}{dt}\lambda_{qs} \quad (4)$$

$$V_{qs} = -R_s i_{qs} - \omega_r \lambda_{ds} + \frac{d}{dt}\lambda_{ds} \quad (5)$$

In the rotor reference frame, the electromagnetic torque (T_e) is given by,

$$T_e = \frac{3P}{2}[\lambda_r i_{qs} - (L_d - L_q) i_{ds} i_{qs}] \quad (6)$$

The rotational speed (ω_r) governed by motion equation is given by,

$$\omega_r = \frac{P}{JS}(T_e - T_m) \quad (7)$$

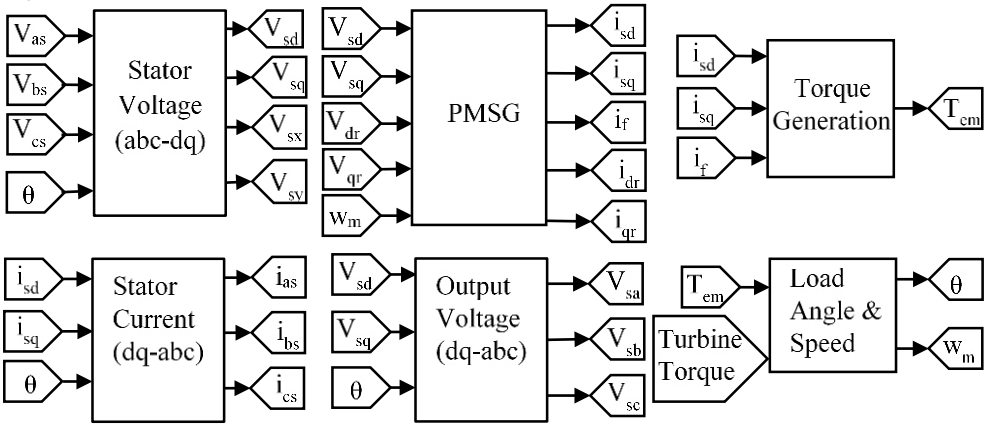

Fig.4: Modelling of PMSG in MATLAB / SIMULINK Environment

4. Design of converter

An AC-DC buck-boost converter is proposed and connected to the output of PMSG and designed to comply with the standard of IEC 61000. The power conversion mainly focuses on standard DC micro-grid, the number of stages involved in power conversion gets reduced. Hence an AC-DC converter system is designed to generate DC power which is independent of frequency and the corresponding design parameters are presented in Table 1.

4.1. Design specifications for AC-DC converter

The output voltage and output current of a 12-pulse rectifier can be expressed by,

$$V_{DC} = \frac{3\sqrt{6}\,V_{ph-ph}}{\pi} \quad (8)$$

$$I_{DC} = \frac{P_{in}}{V_{DC}} \quad (9)$$

Design of input filter for 12-pulse rectifier is given by,

$$\text{Ripple factor } (Rf) = \frac{1}{\sqrt{2}(2f_r RC - 1)} \quad (10)$$

The design equations of the DC-DC converter are given as,

$$V_O = \frac{-D}{1-D} V_{in} \quad (11)$$

The inductor value and capacitor value are given by,

$$L = Vo\frac{(1-D)}{\Delta i_L f_S} \quad (12)$$

$$C = \frac{I_O D}{\Delta V_C f_S} \quad (13)$$

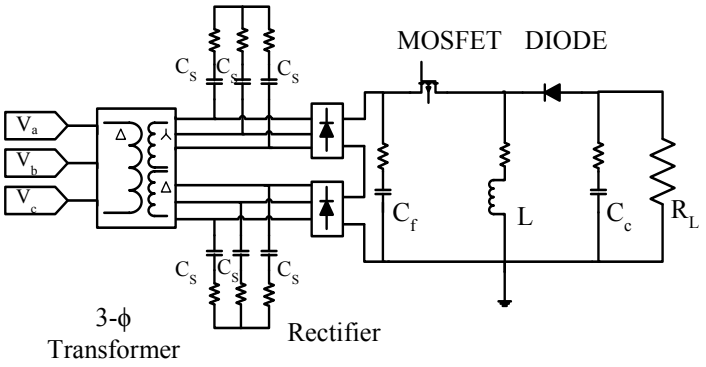

Fig. 5: A schematic diagram of open loop AC-DC buck-boost converter

Table 1: Proposed design parameters for AC-DC buck-boost converter

Parameters	Designed values	
	Buck mode	Boost mode
Duty ratio (D)	20%	60%
Inductor (L)	2.659 mH	25.9 mH
Capacitor (C)	15.19 µF	11.827 µF
Load resistance (R)	10Ω	409Ω
Inductor current (i_L)	47.9 A	22.63 A
Output voltage (V_o)	380 V	2435 V

5. Design of controllers

The dynamic variations of load can be controlled by properly designing an appropriate both proportional integral (PI) and a sliding mode controller (SMC) for buck-boost DC-DC converter to ensure stability of the system under any operating condition, a schematic representation of the PI controller and SM controller for the buck-boost converter is shown in Fig. 6(a) and (b). The gain values K_P, and K_i for PI controller whereas K_1, K_2, K_3 and K_4 for SMC are adjusted to get the desired controlled output for a buck-boost converter.

5.1. Design of PI controller

The dynamic variations of load can be controlled by properly designing an appropriate both proportional integral (PI) and proportional integral derivate (PID) controllers to achieve the desired controller parameters for efficient voltage and current control in a buck-boost converter, the output transfer functions for both voltage and current control [10] is specified by the equations below,

For voltage and current control,

$$GV_C(S) = \frac{v_c(s)}{d(s)} = -\frac{(v_{in}-v_c)}{D'}\frac{\left[1-\frac{sLI}{D'(v_{in}-v_c)}\right]}{\left[1+\frac{sL}{D'^2R}+\frac{s^2LC}{D'^2}\right]}, \text{ and } GI_L(S) = \frac{\iota_L(s)}{d(s)} = \frac{(v_{in}(1+D)}{RD'^3}\frac{\left[1+sC\frac{R}{(1+D)}\right]}{\left[1+\frac{sL}{D'^2R}+\frac{s^2LC}{D'^2}\right]} \quad (14)$$

5.2. Design of SMC

Sliding mode controller is widely used in an engineering application as it uses for exact mathematical representation[11]. It is a nonlinear control technique that adapts the dynamics of the system to slide on the cross-section of a system's normal performance with an interrupted signal. A state-space average approach is important for the mathematical modelling of sliding mode controller[11][12].

Under continuous conduction mode operation of the system [12] state-space averaging model, we will be,

$$\dot{x_1} = -\frac{(1-d)}{L}x_2 - \frac{d}{L}V_{in}$$
$$\dot{x_2} = -\frac{(1-d)}{C}x_1 - \frac{1}{CR}x_2 \quad (15)$$

SMC scheme uses a combination of an input voltage, inductor current and output voltage as tracking error input to SMC. To design a sliding surface, control law will direct the trajectories of the state variables to slide along the sliding surface [13] and the total tracking error state variables trajectory can be expressed as;

$$S = \alpha_1 x_1 + \alpha_2 x_2 + \alpha_3 x_3 \quad (16)$$

From the appropriate sliding mode control law, we can obtain a suitable switching function for the buck-boost converter is as follows;

$$\dot{x}_e > 0, \text{ if } S > 0$$
$$\dot{x}_e < 0, \text{ if } S < 0 \quad (17)$$

In this paper, SMC is designed to control the output voltage of the buck-boost converter by taking input voltage, inductor current and output voltage as state feedback to obtain controlled switching action and it can be expressed as;

$$\hat{d} = \frac{x_e}{x_e - V_{in}} \quad (18)$$

5.3. Performance analysis of control strategies

In this paper performance and comparative analysis of different control techniques is analysed using time and frequency response under load voltage variation as shown in Fig. 8 (a) and (b). Table 2 shows controller parameters with all stability margin for both the controller.

6. Simulation results

Fig. 9(a) and (b) shows the simulated results of a buck-boost converter output voltage and current without a controller in both the modes. A performance of the controllers is analysed under load variation ranging up to 20Ω in buck mode and up to 500Ω in boost mode for a period of 0.3 to 0.6 sec.

As expected output voltage remains the same with a minimum sustained oscillation irrespective of load variation. Fig. 10 (a) and (b) depicts the controlled output voltage and current waveform of a converter using the PI controller for buck and boost mode respectively. Fig. 11 (a) and (b) depicts the controlled output voltage and current waveform of a converter using SMC for buck and boost mode respectively.

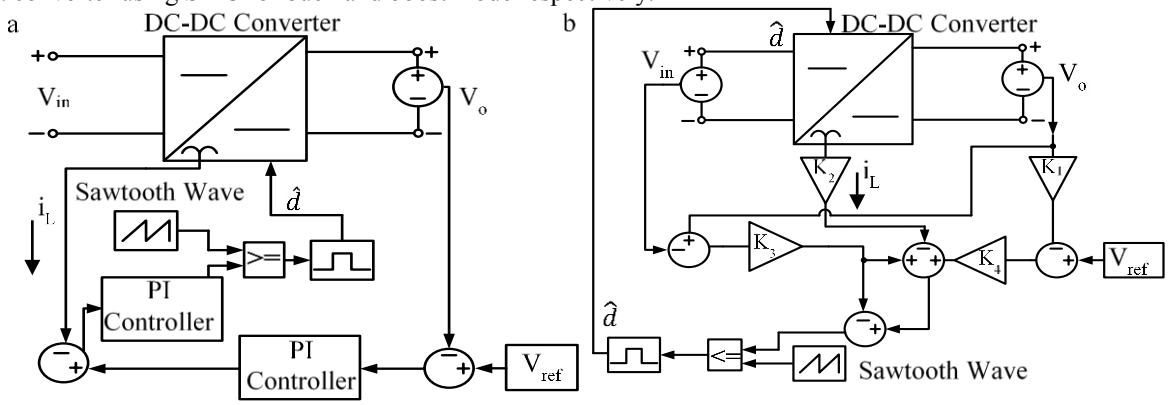

Fig.6 a) A schematic of PI controller for a buck-boost converter, b) A schematic of SMC for a buck-boost converter

Table 2: Controlled parameters for PI controller and SMC

Control strategy	Rise time (sec.)	Settling time (sec.)	Overshoot (%)	Phase margin (dB)	ω_{PM} (rad/sec.)	Gain margin (dB)	ω_{GM} (rad/sec.)
PI controller	0.000322	0.0386	270	Inf	Inf	40.8	0
						19	693
SMC	0.000776	0.0357	78.9	171	909	Inf	Inf
				18.3	1.78E3		

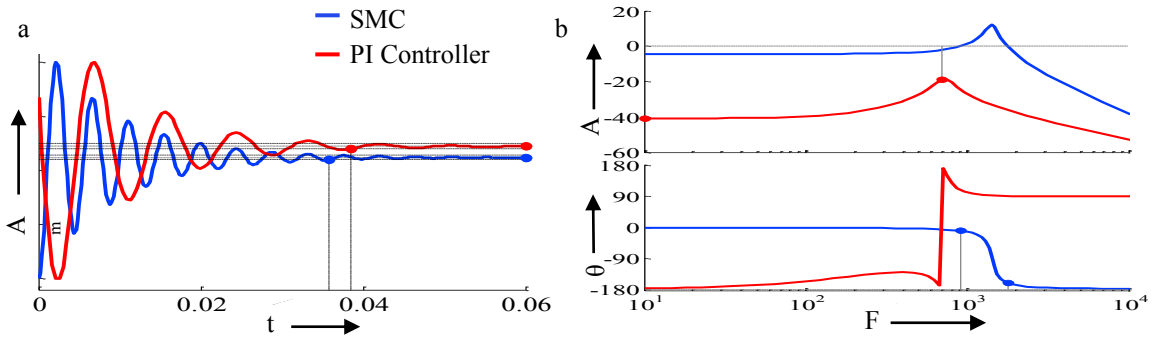

Fig. 7 (a) Comparative step response for PI and SM controller, (b) Comparative bode plot for PI and SM controller.

7. Conclusion

The conventional small-scale TTCS is developed and demonstrated for a converter with the controller and the tidal turbine is modelled using BEM for which the turbine diameter is assumed to be 1.9 m at a marine current speed of 3 m/s. In the DC-DC converter, input and load variation adapt the normal functioning of the system which may harm the overall TTCS, hence control strategy are analysed under load variation by keeping input side consistent and with time and frequency response of the controller. From simulation results, it inferred that an SMC has less settling time, rise time and overshoot as compared to the conventional PI controller. From an output result, it is concluded that SMC is most suitable for robust and non-linear system and provides good voltage regulation and the output voltage is boosted more as compared to the PI controller. In the case of linear control and medium power

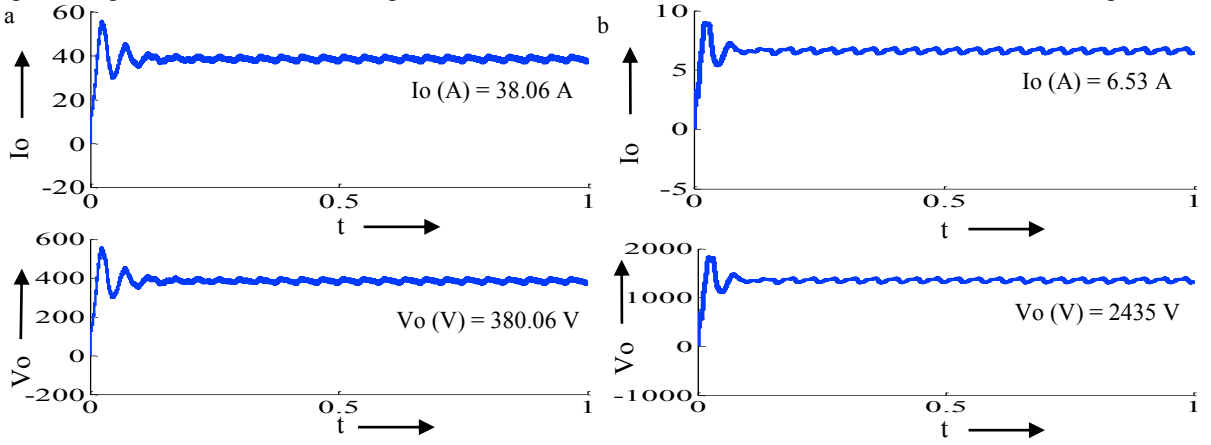

Fig. 8:(a) Output voltage and current of a converter in buck mode, (b) Output voltage and current of a converter in boost mode.

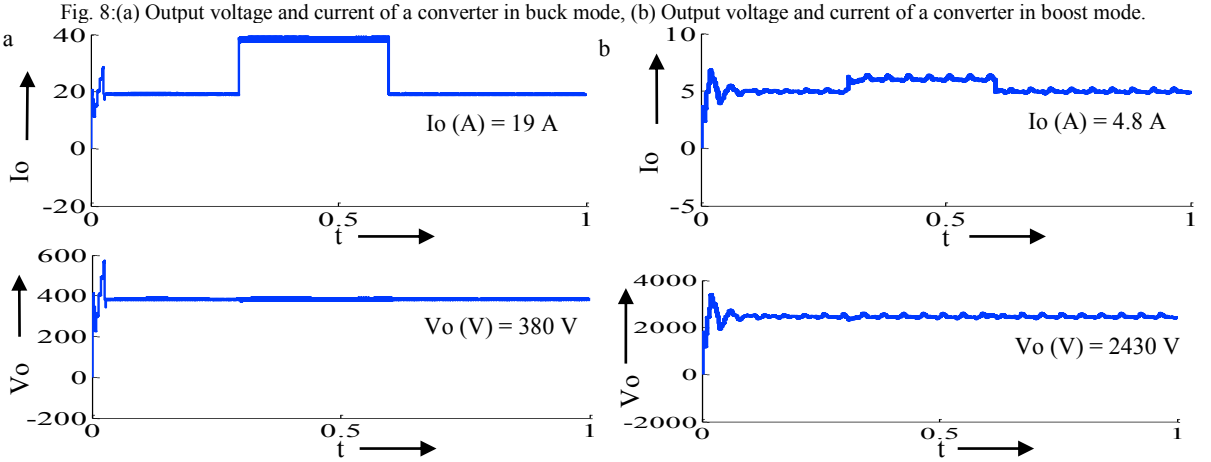

Fig. 9: (a)Controlled output voltage and current of a converter using a PI controller – buck mode, (b)Controlled output voltage and current of a

converter using a PI controller - boost mode.

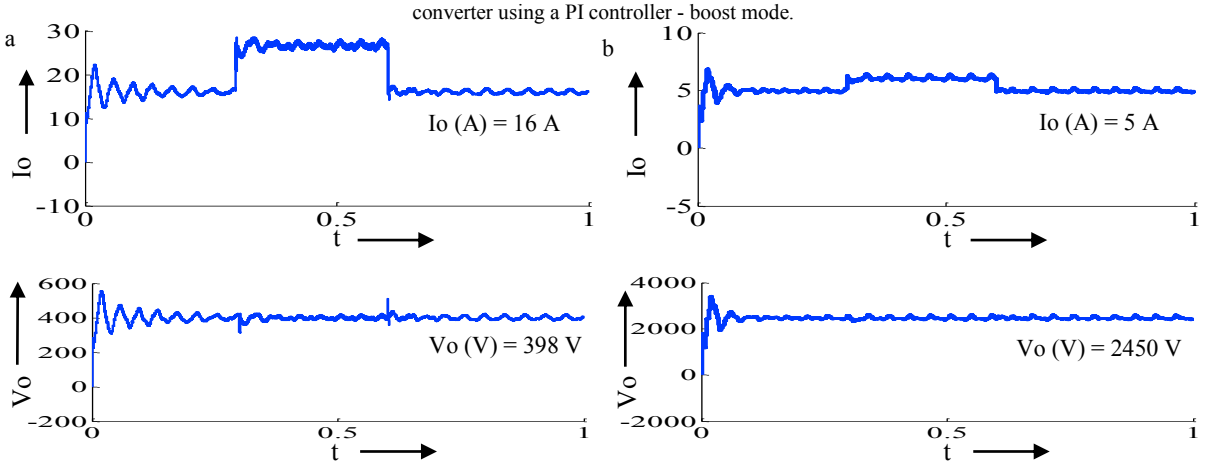

Fig. 10: (a)Controlled output voltage and current of a converter using SMC -buck mode, (b)Controlled output voltage and current of a converter using SMC - boost mode.

application PI controller is recommended, whereas for non-linear control and high-power application SMC is recommended. Further work is underway to include a temporal hydrodynamic response of the turbine to water current fluctuations.

Acknowledgments

The authors would like to thank DST-UKIERI and DST-KNRF/OEC/17-18/137/DSTX/ABDU for the financial support to carry out this research.

References

[1] R. Martinez, G.S. Payne, T. Bruce. "The effects of oblique waves and currents on the loadings and performance of tidal turbines." *Ocean Engineering* 164 (2018): 55–64, doi:10.1016/j.oceaneng.2018.05.057.

[2] M.J. Khan, G. Bhuyan, M.T. Iqbal, J.E. Quaicoe. "Hydrokinetic energy conversion systems and assessment of horizontal and vertical axis turbines for river and tidal applications: A technology status review." *Applied Energy* 86 (2009): 1823–1835, doi:10.1016/j.apenergy.2009.02.017.

[3] E. Ebrahimzadeh, F. Blaabjerg, X. Wang, C.L. Bak. "Harmonic stability and resonance analysis in large PMSG-based wind power plants." *IEEE Transactions on Sustainable Energy* 9 (2018): 12–23, doi:10.1109/TSTE.2017.2712098.

[4] T. Korakianitis, M.A. Rezaienia, X. Shen, E.J. Avital, A. Munjiza, P.H. Wen, J.J.R. Williams. "Aerodynamics of wind turbine technology." in *Handbook of Clean Energy Systems*, John Wiley & Sons, Ltd, London, UK, (2015): 1–22, doi:10.1002/9781118991978.hces046.

[5] K. Ai, E.J. Avital, T. Korakianitis, A. Samad, N. Venkatesan. "Surface wave effect on marine current turbine, modelling and analysis." in Proceedings of 2016 7th *International Conference on Mechanical and Aerospace Engineering,* ICMAE 2016, London, UK, (2016): 180–184, doi:10.1109/ICMAE.2016.7549531.

[6] X. Bai, E.J. Avital, A. Munjiza, J.J.R. Williams. "Numerical simulation of a marine current turbine in free surface flow." *Renewable Energy* 63 (2014): 715–723, doi:10.1016/j.renene.2013.09.042.

[7] A.S. B. Meghni, D. Dib, Ahmad T. Azar. "Effective supervisory controller to extend optimal energy management in hybrid wind turbine under energy and reliability constraints." *International Journal of Dynamics and Control* 6 (2017): 369–383, doi:10.1007/s40435-016-0296-0.

[8] O. Elbeji, M. Ben Hamed, L. Sbita. "PMSG wind energy conversion system: modeling and control." I*nternational Journal of Modern Nonlinear Theory and Application* 03 (2014): 88–97, doi:10.4236/ijmnta.2014.33011.

[9] A.G. A. Sahu, A.K. Bhoi, K.S. Sherpa. "Modelling of a permanent magnet synchronous generator based wind energy conversion system." in *Advances in Smart Grid and Renewable Energy,* S. SenGupt, Springer Nature Singapore Pte Ltd. (2018): 23–32, doi:10.1007/978-981-10-4286-7_3.

[10] D.S. Wijeratne, G. Moschopoulos. "A novel three-phase buck-boost ac-dc converter." *IEEE Transactions on Power Electronics* 29 (2014): 1331–1343, doi:10.1109/TPEL.2013.2260563.

[11] M. Gao, D. Wang, Y. Li, T. Yuan. "Fixed frequency pulse-width modulation based integrated sliding mode controller for phase-shifted full-bridge converters." *IEEE Access* 6 (2018): 2181–2192, doi:10.1109/ACCESS.2017.2782225.

[12] S. Ding, W.X. Zheng, J. Sun, J. Wang. "Second-order sliding-mode controller design and its implementation for buck converters." *IEEE Transactions on Industrial Informatics* 14 (2018): 1–10, doi:10.1109/TII.2017.2758263.

[13] L. Ma, Y. Zhang, X. Yang, S. Ding, L. Dong. "Quasi-continuous second-order sliding mode control of buck converter." *IEEE Access* 6 (2018): 1–8, doi:10.1109/ACCESS.2018.2795027.